


Feasibility of Treatment Planning System in Localizing the COVID-19 Pneumonia Lesions and Evaluation of Volume Indices of Lung Involvement

Dose-Response:
An International Journal
July-September 2020:1-8
© The Author(s) 2020
Article reuse guidelines:
sagepub.com/journals-permissions
DOI: 10.1177/1559325820962600
journals.sagepub.com/home/dos



Ruhollah Ghahramani-Asl^{1,2}, Pejman Porouhan³, Mohammad Mehrpouyan¹, James S. Welsh⁴, Edward J. Calabrese⁵ , Rachna Kapoor⁶, Gaurav Dhawan⁷ , and Seyed Alireza Javadinia⁸ 

Abstract

Background and purpose: To assess the feasibility of a treatment planning system in localizing, contouring, and targeting lung lesions along with an evaluation of volume indices of lung involvement in patients with COVID-19 pneumonia.

Methods: We evaluated 10 patients with PCR-confirmed COVID-19 pneumonia. The CT images were imported into the ISOgray[®] treatment planning system to anatomically define and contour the volumes of the pulmonary lesions, the lungs, and other nearby organs.

Results: The ratio of lung lesion volume to lung volume in this study was 0.11 ± 0.13 (11.13%). The highest mean biosynthesis ratio of lung lesions was 0.36. The ratio of lesion volume in the left lung of patients with the highest volume of involvement, was 0.44, and the ratio of lesion volume in the right lung of these patients was 0.27 (approximately 1.5 times more in the left lung than the right lung). On average, CTDIvol and DLP for all patients studied in our study were 11.22 ± 2.47 mGy and 354.20 ± 65.11 mGy.cm

Conclusion: We reported the feasibility of using a treatment planning system in localizing COVID-19 pulmonary lesions and its validity in the volumetric assessment of infected lung regions.

Keywords

low dose radiotherapy, treatment planning system, 3 dimensional (3D) conformal radiation therapy, COVID-19, SARS-CoV-2, acute respiratory distress syndrome (ARDS)

Introduction

The novel coronavirus, SARS-CoV-2, emerged in late 2019 and quickly led to a worldwide pandemic in early 2020. The

most common symptoms of this disease, known as COVID-19, are fever and chills, dry cough, fatigue, sputum production, dyspnea, pharyngitis, cephalgia, and myalgia. However, this

¹ Department of Medical Physics and Radiation Sciences, Faculty of Paramedicine, Sabzevar University of Medical Sciences, Sabzevar, Iran

² Clinical Research Development Unit, Hospital Research Development Committee, Sabzevar University of Medical Sciences, Sabzevar, Iran

³ Department of Radiation Oncology, Vasei Educational Hospital, Sabzevar University of Medical Sciences, Sabzevar, Iran

⁴ Loyola University Chicago, Edward Hines Jr., VA Hospital, Stritch School of Medicine, Department of Radiation Oncology, Maywood, IL, USA

⁵ Department of Environmental Health Sciences, School of Public Health and Health Sciences, University of Massachusetts, Amherst, MA, USA

⁶ Saint Francis Hospital and Medical Center, Hartford, CT, USA

⁷ MedSurg Urgent Care, Gilbertsville, PA, USA

⁸ Cellular and Molecular Research Center, Sabzevar University of Medical Sciences, Sabzevar, Iran

Received 14 June 2020; received revised 31 August 2020; accepted 31 August 2020

Corresponding Author:

Seyed Alireza Javadinia, Vasei Educational Hospital, TohidShar BLV, Sabzevar, Razavi Khorasan, 9617747431, Iran.
Emails: javadinia.alireza@gmail.com; javadinia941@mums.ac.ir



Creative Commons Non Commercial CC BY-NC: This article is distributed under the terms of the Creative Commons Attribution-NonCommercial 4.0 License (<https://creativecommons.org/licenses/by-nc/4.0/>) which permits non-commercial use, reproduction and distribution of the work without further permission provided the original work is attributed as specified on the SAGE and Open Access pages (<https://us.sagepub.com/en-us/nam/open-access-at-sage>).

disease initially affects patients' pulmonary function, which can range from asymptomatic (mere evidence of involvement on CT scans of the lungs) to very severe cases and even death. Although there is less than a 15 percent chance of developing lung complications such as pneumonia, according to current evidence, severe complications and irreversible respiratory effects may occur in recovering patients.¹ COVID-19 may induce severe complications in certain population such as elderly patients and people with underlying conditions such as hypertension or diseases such as cancer; are more likely to require admission to intensive care units and have higher mortality rates.²

Low dose radiation therapy (LDRT) has been used previously in the first half of the 20th century to treat several inflammatory and infectious diseases including bacterial/viral pneumonia, bronchial asthma, sinusitis, inner ear infections, pertussis etc.³⁻¹² Since the main manifestation of COVID-19 is pneumonia, several researchers have suggested the potential of using LDRT in the treatment of COVID-19 associated pneumonia and Acute Respiratory Distress Syndrome (ARDS) with cytokine storm. LDRT is known to induce an anti-inflammatory phenotype that results in rapid amelioration of the systemic inflammatory cascade, while avoiding long-term adverse effects.¹³ Several clinical trials are currently underway across the globe to elicit the beneficial effects of LDRT.¹⁴

Computerized tomography (CT) scan is a clinical procedure with high sensitivity and specificity for the diagnosis and determination of pulmonary lesions in patients infected with the COVID-coronavirus.¹⁵ High resolution, one-millimeter-thick slices of the chest, without iodine contrast is a sensitive diagnostic tools in assessment of patients with COVID-19 and the main patterns of involvement are ground-glass opacity (GGO), consolidation, crazy-paving and linear infiltrations.^{16,17} Based on such CT patterns, a lot of anatomical and pathological information, including the volume, location, nature and extent of damage can be deduced. The clinical utility of determining the volume, location, and extent of various pulmonary complications, such as intravascular thromboses and emboli, has been demonstrated from diagnostic images.^{18,19}

In other hand, in radiotherapy, one of the applications of tomographic images (such as diagnostic CT-scan data or CT-simulations (treatment planning CT studies)) is to obtain and evaluate anatomical and pathological data from tumor and normal tissues and then design a CT-based computer treatment plan in order to preserve the normal organs and prescribe the dose to target volumes.²⁰ One of the steps in the computer-based treatment planning process is "contouring," which aims to delineate the contour of the skin and other normal structures, and to locate and volumetrically define the treatment target; all this can be easily obtained from CT images. Also, the photon attenuation information obtained from CT data reveals the electron density of various tissues in the body. Such electron density information is necessary to calculate and plan the dose that will be delivered by the treatment beams. In computer treatment planning systems (TPS) after entering the patient's images, radiation oncologists are able to evaluate 2- and 3-dimensional (3D) anatomical information of the internal

organs, therapeutic volumes, beam's eye view (BEV) radiation fields with different shapes and digitally reconstructed radio-graphs (DRRs) to determine the distribution of therapeutic doses at the desired depth. After such detailed treatment planning and analysis, the optimal treatment plan is selected and sent to the therapeutic machine with the aim of maximizing tumor control and minimizing normal tissue complications. The use of these tools makes it possible for the radiation oncologists and radiation teams to acquire a true 3D volumetric view of the patient and the various targets (and avoidance structures) and a good understanding of the locations of the organs at risk (OARs) relative to the target volumes.

Overall, LDRT in COVID-19 pneumonia can be used as whole lung irradiation (WLI) since diffuse involvement of lungs has been reported in a considerable portion of patients or as localized radiotherapy of COVID-19 pulmonary lesions. Using 3D-conformal radiation therapy (3D-CRT) enables physicians to accurately treat targets and spare organs at risk such as spinal cord. Given that LDRT is one of the proposed treatment strategies for COVID-19 pneumonia and ARDS with cytokine storm, the need to use computer-based treatment planning systems for the 3D-CRT is likely inevitable, especially when pulmonary involvement is localized and without cardiac involvement rather than widespread in some of the patients.

The aim of this study was to assess the feasibility of the treatment planning system in localizing the COVID-19 pneumonia lesions and evaluation of volume indices of lung involvement of infected patients.

Material and Methods

In this prospective cross-sectional study, the demographic information of 10 patients (including 8 men and 2 women with ages ranging from 40 to 75 years), with COVID-19 pneumonia between March 1 and 13, 2020, was examined. The patient inclusion criteria were a positive RT-PCR test from a sample of pharyngeal mucosal swabs and a diagnostic CT scan of thorax before treatment.

Thoracic high-resolution CT scans of patients were taken without contrast injection in the supine position and with respiratory gating. The average imaging parameters were 110 kVp and 130 mAs for all patients. The CT images were imported into the ISOgray[®] treatment planning system (DOSIsoft company, France) to determine the location and contour the volumes of the lesions and the lungs. Contouring or segmentation is an essential process in radiation therapy of the lesions to determine the normal and target volumes such as gross tumor volume (GTV), clinical target volume (CTV), and planning target volume (PTV) performed by a radiation oncologist from the CT images in TPS.

The acquired CT studies allowed 3D anatomical evaluation of patients for treatment planning. Window width and window level settings were adjusted to better visualize involved pulmonary lesions. CT window width (WW) determines the range of CT numbers (or Hounsfield units) displayed on the gray scale in the patient's CT image. The wider the WW, the higher the CT display range. But CT window level determines the CT

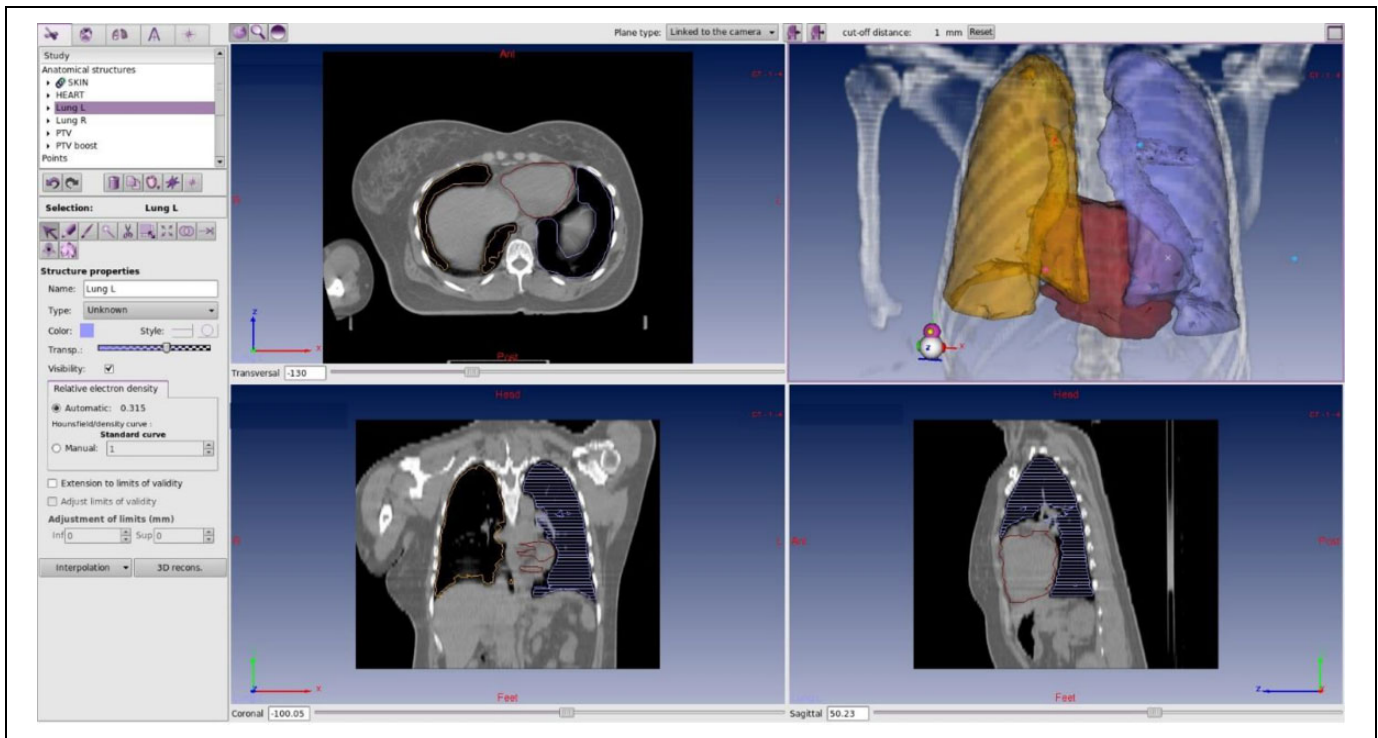


Figure 1. Schematic view for thoracic CT organs contouring of a patient. Contouring can be done manually, semi-automatic and automatically.

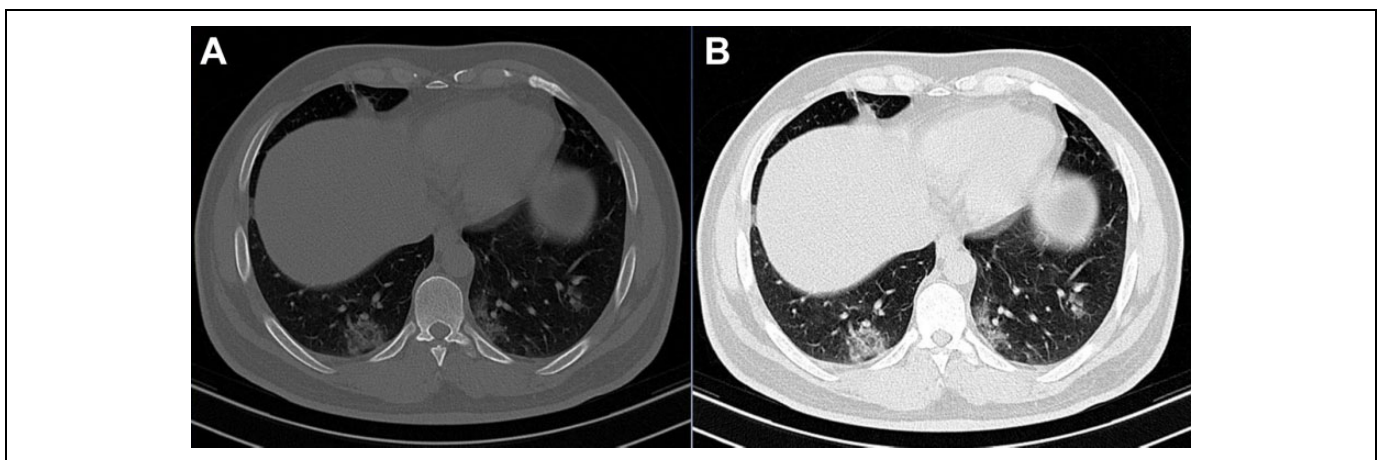


Figure 2. A single transaxial thoracic CT image with bone window (A) and with lung window (B) displayed. Pixel values in window width ranged from 1800 to 2200 for bone and 300 to 1100 for lung.

number of the WW center, or the density and brightness of the image. According to most available sources, window level / width equal to $-400-600\text{HU} / 400-1600\text{HU}$ is used for lung tissue and $0-50\text{HU} / 400-1000\text{HU}$ is used for soft tissue (mediastinum, hila and pleura). These values may be slightly different for different scanners and software platforms and can be selected in consultation with radiation specialists. The CT dose index (CTDIvol) and dose length product (DLP) were also reported as the patient's dose index based on the CT imaging protocol. DLP is the product of CTDIvol multiplication and scan length. The same radiologist interpreted the images and P.P. and S.A.J. contoured the volumes of abnormalities.

To detect pulmonary lesions from COVID-19 pneumonia, window level/width settings equal to the median of $-370/1700$ were used and the lesions were contoured. Lung volumes were drawn semi-automatically (Figure 1). The ratio of lesion volume in each lung to the total volume of the corresponding lung was then determined (Figure 2).

Results

The study was performed using lung CT scan data from 10 patients with a positive PCR test for COVID-19. Demographic information, and information on clinical and laboratory

Table 1. Demographics, Symptoms and Vital Signs of Patients.

Num	Demographics			Symptoms							Vital signs						
	Age	Gender	Comorbidity	Time-interval* (d)	Dry cough	Productive cough	Fever	Sore throat	Headache	Malaise	Shortness of breath	sBP (mmHg)	dBP (mmHg)	SpO2 (%)	HR (bpm)	RR (breaths/min)	Temp (°C)
1	46	M	0	2	Y	N	Y	N	N	N	N	130	80	92	112	24	37.5
2	68	M	0	5	Y	N	Y	N	N	Y	Y	130	80	85	85	20	37.5
3	40	M	0	3	Y	N	Y	N	N	Y	Y	130	80	98	114	20	37.5
4	75	F	DM, HTN	1	Y	N	Y	N	N	Y	Y	160	80	89	86	18	37
5	75	M	DM, HTN	7	Y	N	N	N	N	Y	Y	110	80	90	79	18	36.5
6	42	F	0	10	Y	N	Y	N	N	Y	Y	130	80	96	127	20	36.5
7	34	M	0	2	Y	N	N	N	N	Y	Y	115	70	97	75	21	36.8
8	42	M	0	7	Y	N	Y	N	Y	Y	Y	100	60	86	96	20	37.3
9	52	M	0	1	Y	N	Y	N	N	Y	Y	120	80	95	84	16	38
10	38	M	0	5	Y	N	N	N	N	Y	Y	130	80	85	85	20	39.5

* to admission after the onset of symptoms.

M: male, F: female, Y: yes, N: No, sBP: systolic blood pressure, dBP: diastolic blood pressure, bpm: beats per minute SpO2: oxygen saturation levels, HR: heart rate, RR: respiratory rate, Temp: Temperature, DM: diabetes mellitus, HTN: hypertension.

Table 2. Laboratory Tests and Imaging Characteristics of Patients.

Num	Lab test										Imaging values				
	PCR	WBC $\times 10^9/L$	Neu (%)	Lym (%)	HgB (g/dl)	ESR (mm/h)	CRP*	Consolidation	GGO	Bilateral lung involvement	Number of lesions	Pleural effusion	Lymphadenopathy	Calcification	
1	Y	4.400	0.78	0.19	12.4	55	3	N	Y	Localized	N	N	N	N	
2	Y	6.100	0.9	0.09	13	20	3	N	Y	Wide spread	N	N	N	N	
3	Y	8.300	0.9	0.06	12	51	3	N	Y	Wide spread	N	N	N	N	
4	Y	5.700	0.6	0.33	11.6	26	3	N	Y	Wide spread	N	N	N	N	
5	Y	6.000	0.79	0.17	13.2	8	0	N	Y	Wide spread	N	N	N	N	
6	Y	5.400	0.61	0.36	11.2	24	0	N	Y	Wide spread	N	N	N	N	
7	Y	4.600	0.52	0.45	14.4	29	2	N	Y	Wide spread	N	N	N	N	
8	Y	5.700	0.74	0.24	14.2	25	0	Y	Y	Wide spread	N	N	N	N	
9	Y	9.800	0.8	0.17	12.7	31	3	Y	Y	Localized	N	N	N	N	
10	Y	8.300	0.9	0.06	12	51	3	N	Y	Wide spread	N	N	N	N	

* Qualitative assessment.

PCR: polymerase chain reaction, WBC: white blood cells, Neu: Neutrophils, Lym: lymphocytes, HgB: hemoglobin, ESR: erythrocyte sedimentation rate, CRP: C-reactive protein, GGO: Ground glass opacities.

Table 3. CT Image Quantification and Dosimetric Values of Patients.

Number	Lesions.L (cm ³)	Lung.L (cm ³)	Lesions.R (cm ³)	Lung.R (cm ³)	Ratio.L	Ratio.R	Involvement (%)	CTDI (mGy)	DLP (mGy.cm)
1	28.64	1449.38	76.05	1565.67	0.02	0.05	3.42	11.6	371
2	196.22	1695.04	221.73	1951.11	0.12	0.11	11.47	11.8	380
3	53.48	1168	19.01	1519	0.05	0.01	2.92	11.89	362
4	127.9	913.53	26.41	1303.87	0.14	0.02	8.01	11.33	315
5	503.91	1139.22	376.94	1403.19	0.44	0.27	35.55	9.9	318
6	41.93	1524.41	9.83	1773.03	0.03	0.01	1.65	10.1	321
7	62.17	1964.18	161.48	2474.77	0.03	0.07	4.85	13.27	417
8	207.95	2123.94	249.54	2524.95	0.10	0.10	9.84	9.39	341
9	0	2037.14	158.26	1925.99	0.00	0.08	4.11	6.78	238
10	615.39	1436.48	364.94	1682.17	0.43	0.22	32.27	16.09	479

L: left, R: Right, CTDI: CT dose index, DLP: dose length product.

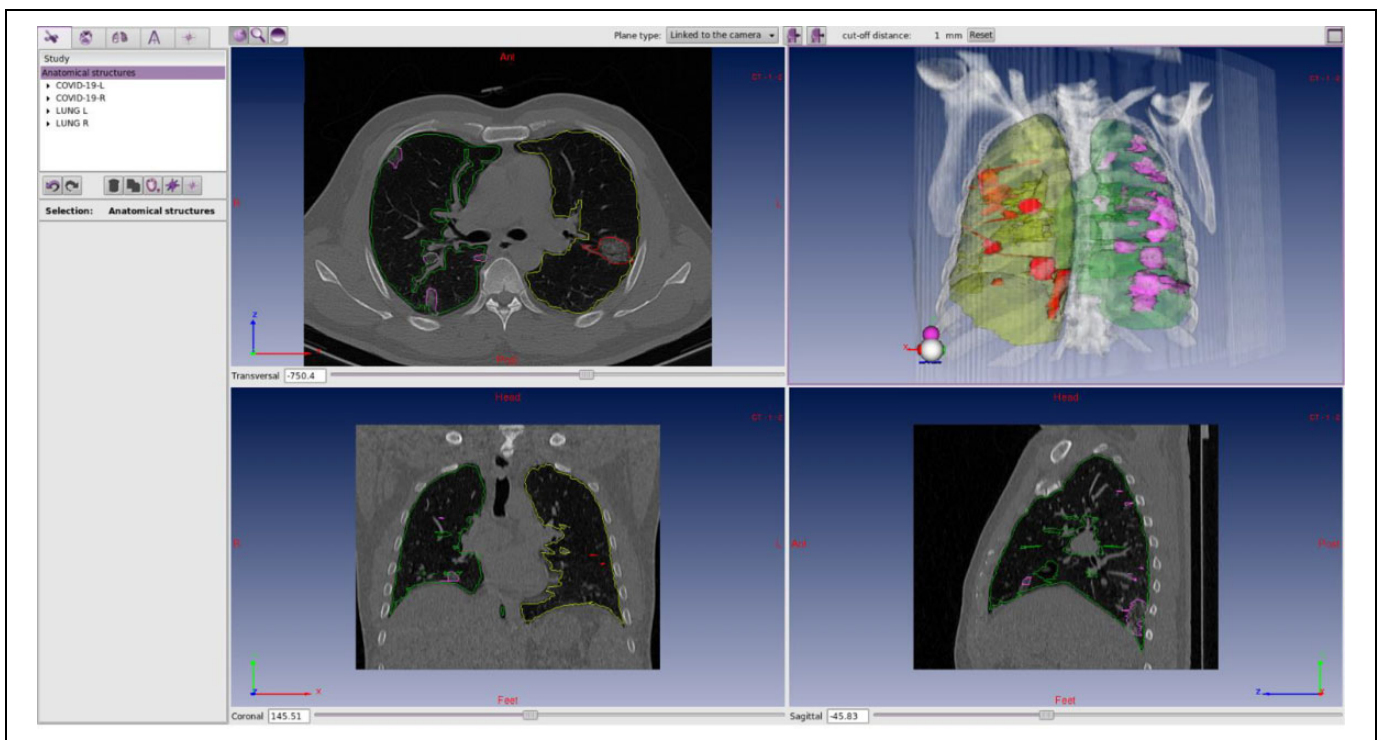


Figure 3. The images of the first COVID-19 patient with low grade lung involvement. The volumes of lesions in the left and right lungs were 28.64 and 76.05 cm³ respectively. The acquired sum ratio for this volume involvements was 0.07 (or 7%).

findings are shown in Tables 1 and 2. Most of the patients were male (80%) and had no underlying disease (80%). The most common symptoms in the patients were cough and dyspnea, which were present in all patients. In terms of vital signs, all patients were stable at baseline. The most common finding in imaging patients was GGO lesions, which were bilateral in 90% of cases.

To quantitatively analyze CT data, the volume of pulmonary lesions obtained in the left and right lungs of all patients with their ratio to the total volume of each lung is presented in Table 3. In general, the mean ratio of lung lesion volume to lung volume in the patients studied in this study was 11.13%. The maximum mean biosynthesis ratios of lung lesions were 0.36 and 0.32 (respectively for patients No. 5 and 10) and the

minimum mean was 0.2 and 0.3 (for patients No. 6 and 1, respectively). The ratio of lesion volume in the left lung of patients with the highest volume of involvement, i.e. patients No.5 and 10, was 0.44 and 0.43, and the ratio of lesion volume in the right lung of these patients was 0.27 and 0.22 (approximately 1.5 times more for the left lung than the right lung). In general, the mean lung lesion volume ratio for the left lung was slightly higher in most patients than in the right lung (0.13 ± 0.16 versus 0.09 ± 0.09). Also, the ratio of lung lesion volume to lung volume in female patients was lower than male patients (0.05 ± 0.04 versus 0.13 ± 0.13).

The highest volume of pulmonary lesions was found in the left lungs of patients No. 5 and 10, which were measured at 503.9 and 615.39 cm³, respectively. The lowest lesion volume

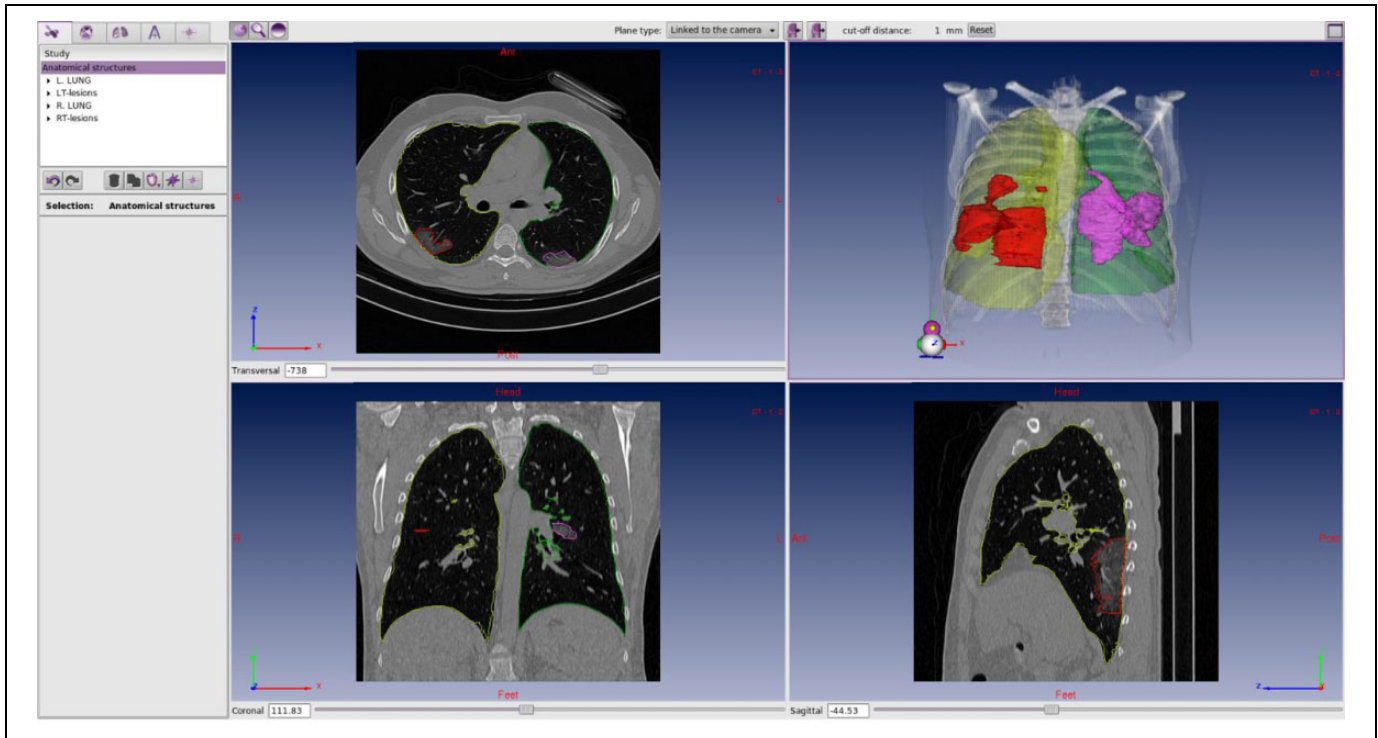


Figure 4. The images of the **eighth** COVID-19 patient with moderate grade lung involvement. The volumes of lesions in the left and right lungs were 207.95 and 249.54 cm³ respectively. The acquired sum ratio for this volume involvements was 0.20 (or 20%).

was observed in the right lungs of patients No. 3 and 6, which were 19.01 and 9.83 cm³, respectively. It is noteworthy that no lesions were observed in the left lung of patient No. 9. Among all patients, the total lung lesion volume of was 71% and was present in the oldest male patient aged 75 years (patient No. 5).

On average, CTDI_{vol} and DLP for all patients studied in our study were 11.22 ± 2.47 mGy and 354.20 ± 65.11 mGy.cm, respectively (Table 3).

Figures 3-5 show the contoured images of COVID-19 patients with low, moderate, and severe lung involvement.

Discussion

In the present study, using contouring software (i.e. the treatment planning system or TPS), even very small pulmonary lesions and small involved volumes of COVID-19 patients were readily detected and contoured by the software. In this study, the percentage of lung involvement with COVID-19 pneumonia was 11.41%. Bernheim et al. showed that the extent of pulmonary involvement in COVID-19 patients was generally modest (mean score of 3 out of a maximum score of 20) similar to the findings of present study.²¹ Contrary to the findings of these 2 studies, Caruso et al. reported extensive pulmonary involvement in most of their COVID-19 patients.²² The observed difference is probably due to the time of obtaining the lung imaging (as we performed only at presentation) and also the age group of patients. Ground glass opacities (GGO) were observed in all patients and bilateral involvement

was reported in 90% of patients. These findings are consistent with previous reports on imaging features of patients with COVID-19.²³

The mean CTDI_{vol} and DLP measurements for patients in our study were 11.22 ± 2.47 mGy and 354.20 ± 65.11 mGy.cm, respectively. According to the current evidence, the dose received to the patient's organs by the CT studies depends on the volume computed tomography dose index, the scanner input length, and the size of the patient. For instance, when performing chest CT with CTDI_{vol} equal to 10 mGy, the dose reached to the lung tissue of a person weighing 100 kg is equal to 10 mGy, a person weighing 75 kg is equal to 15 mGy and a person weighing 45 kg is equal to 20 mGy which is approximately consistent with values reported in the present study.²⁴

Besides the interesting potential of the treatment planning system in volumetric assessment of COVID-19 pneumonia lesions and its possible diagnostic and prognostic role in determining the severity of disease, some researchers have proposed a role for low dose radiation therapy in the treatment of COVID-19-induced acute respiratory distress syndrome (ARDS).²⁵ Although much controversy persists, because of the absence of clearly effective preferred treatment options for COVID-19, low dose radiation therapy may be considered in selected cases.^{13,25-27} Because the pulmonary involvement is not always widespread, involved-field radiotherapy may minimize potential side effects. In this context, using computerized treatment planning systems is the best option. In this study, for the first time, we reported that the treatment planning system

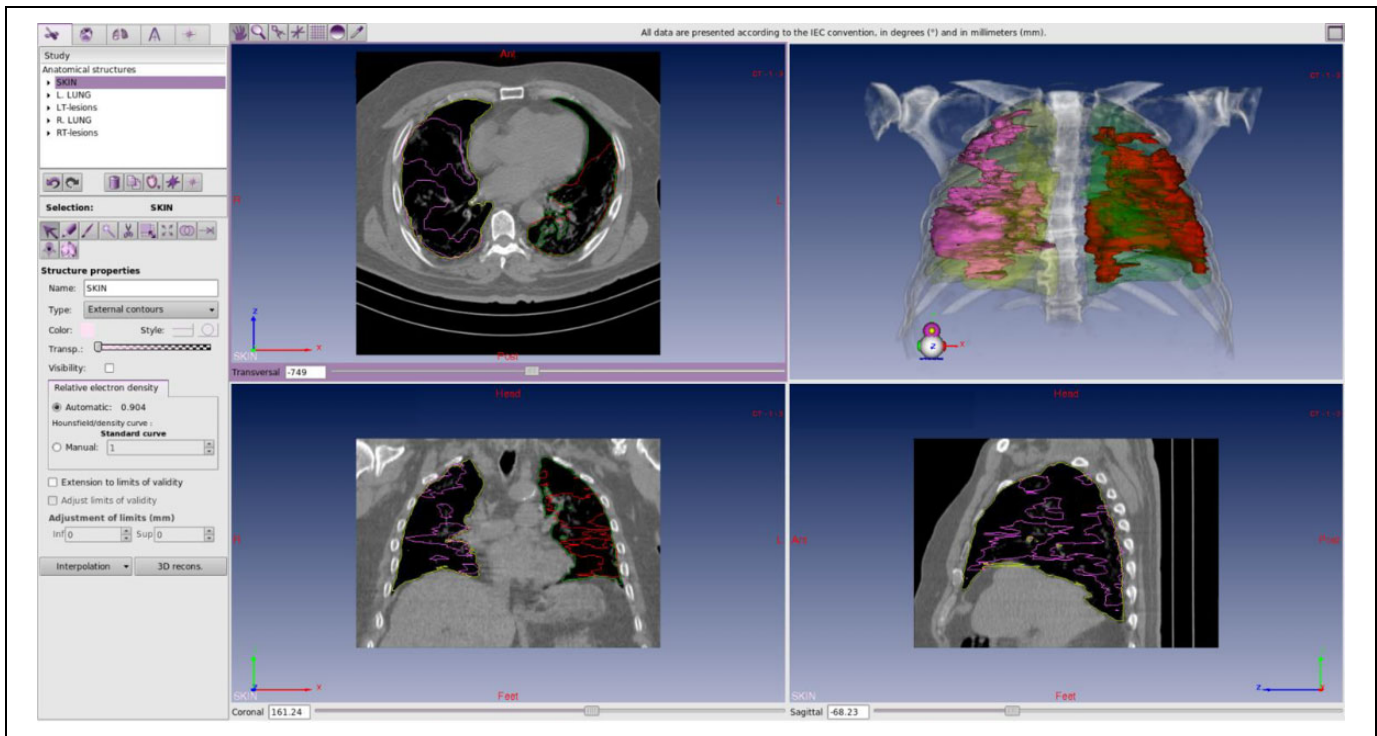


Figure 5. The images of the **fifth** COVID-19 patient with severe grade lung involvement. The volumes of lesions in the left and right lungs were 503.91 and 376.94 cm³ respectively. The acquired sum ratio for this volume involvements was 0.71 (or 71%).

can be successfully used in volumetric assessment of COVID-19 lung lesions and that it is a valid tool in determining the location of pulmonary lesions. These volumes can potentially be used for low dose radiation therapy treatment planning, although the proper margins for clinical target volume (CTV) determination should be addressed in future studies.

Conclusions

In this study, for the first time, we report the feasibility and acceptability of using the treatment planning system in volumetric assessment of COVID-19 lung lesions and its validity in determining the location of pulmonary lesions as a target for 3D conformal radiation therapy. As the possible role of low dose radiation therapy for COVID-19 pneumonia evolves, the findings of this present study may prove valuable for partial lung irradiation (if that strategy ever proves to be a viable option).

Authors' Note

The protocol of study was approved by the University Research Ethics Committee of Sabzevar University of Medical Sciences [IR.MED-SAB.REC.1399.016]. Informed rewritten consent form was obtained from each patient before beginning of study.

Acknowledgments

We thank all the frontline healthcare professionals who are fighting against COVID-19. We also appreciate the Clinical Research Development Unit, Hospital Research Development Committee, Sabzevar

University of Medical Sciences. E.J.C. acknowledges longtime support from the US Air Force (AFOSR FA9550-13-1-0047) and Exxon-Mobil Foundation (S1820000000256).




Declaration of Conflicting Interests

The author(s) declared no potential conflicts of interest with respect to the research, authorship, and/or publication of this article.

Funding

The author(s) disclosed receipt of the following financial support for the research, authorship, and/or publication of this article: This work was supported by Sabzevar University of Medical Sciences [grant number 99003;2020. Recipient: Ruhollah Ghahramani-Asl].

ORCID iD

Edward J. Calabrese  <https://orcid.org/0000-0002-7659-412X>
 Gaurav Dhawan  <https://orcid.org/0000-0003-0511-7323>
 Seyed Alireza Javadinia  <https://orcid.org/0000-0003-2467-837X>

References

1. World Health Organization. Report of the WHO-China Joint Mission on Coronavirus Disease 2019 (COVID-19). February; 2020.
2. Zhang L, Zhu F, Xie L, et al. Clinical characteristics of COVID-19-infected cancer patients: a retrospective case study in three hospitals within Wuhan, China. *Ann Oncol.* 2020;31(7): 894-901. doi:10.1016/j.annonc.2020.03.296
3. Calabrese EJ. X-Ray treatment of carbuncles and furuncles (boils): a historical assessment. *Hum Exp Toxicol.* 2013;32(8): 817-827. doi:10.1177/0960327112467046 [PubMed:23821639].

4. Calabrese EJ, Dhawan G. The role of x-rays in the treatment of gas gangrene: a historical assessment. *Dose-Response*. 2012; 10(4):626-643. doi:10.2203/dose-response.12-016.Calabrese [PubMed:23304109].
5. Calabrese EJ, Dhawan G. How radiotherapy was historically used to treat pneumonia: could it be useful today? *Yale J Biol Med*. 2013;86(4):555-570. [PubMed:24348219].
6. Calabrese EJ, Dhawan G. The historical use of radiotherapy in the treatment of sinus infections. *Dose-Response*. 2013;11(4): 469-479. doi:10.2203/dose-response.13-004.Calabrese [PubMed: 24298225].
7. Calabrese EJ, Dhawan G. Historical use of x-rays: treatment of inner ear infections and prevention of deafness. *Hum Exp Toxicol*. 2014;33(5):542-553. doi:10.1177/0960327113493303 [PubMed: 23800998].
8. Calabrese EJ, Dhawan G, Kapoor R. Use of X-rays to treat shoulder tendonitis/bursitis: a historical assessment. *Arch Toxicol*. 2014;88(8):1503-1517. doi:10.1007/s00204-014-1295-6 [PubMed:24954447].
9. Calabrese EJ, Dhawan G, Kapoor R. The use of x rays in the treatment of bronchial asthma: a historical assessment. *Radiat Res*. 2015;184(2):180-192. doi:10.1667/rr14080.1 [PubMed: 26207685].
10. Calabrese EJ, Dhawan G, Kapoor R. Radiotherapy for pertussis: an historical assessment. *Dose-Response*. 2017;15(2): 1559325817704760. doi:10.1177/1559325817704760 [PubMed: 28529467].
11. Calabrese EJ, Dhawan G, Kapoor R, Kozumbo WJ. Radiotherapy treatment of human inflammatory diseases and conditions: optimal dose. *Hum Exp Toxicol*. 2019;38(8):888-898. doi:10.1177/ 0960327119846925 [PubMed:31060383].
12. Dhawan G, Kapoor R, Dhamija A, Singh R, Monga B, Calabrese EJ. Necrotizing fasciitis: low-dose radiotherapy as a potential adjunct treatment. *Dose-Response*. 2019;17(3):1559325819871757. doi:10.1177/1559325819871757 [PubMed:31496924].
13. Dhawan G, Kapoor R, Dhawan R, et al. Low dose radiation therapy as a potential life saving treatment for COVID-19-induced acute respiratory distress syndrome (ARDS). *Radiother Oncol*. 2020;147:212-216.
14. The National Library of Medicine (NLM) Clinical Trials Gov. 2020. Accessed June 14, 2020. [https://clinicaltrials.gov/ct2/re-](https://clinicaltrials.gov/ct2/results?cond=COVID&term=low+dose+radiation&entry=&state=&city=&dist=)
15. Majidi H, Niksolat F. Chest CT in patients suspected of COVID-19 infection: a reliable alternative for RT-PCR. *Am J Emerg Med*. 2020;S0735-6757(20):30244-30248. doi:10.1016/j.ajem.2020.04. 016 [PubMed:32312575].
16. Ai T, Yang Z, Hou H, et al. Correlation of chest CT and RT-PCR testing in coronavirus disease 2019 (COVID-19) in China: a report of 1014 cases. *Radiology*. 2020;296(2):E32-E40. doi:10.1148/radiol.2020200642 [PubMed:32101510].
17. Fang Y, Zhang H, Xie J, et al. Sensitivity of chest CT for COVID-19: comparison to RT-PCR. *Radiology*. 2020;296(2): E115-E117.
18. Kanne JP, Chest CT. Findings in 2019 novel coronavirus (2019-nCoV) infections from Wuhan, China: key points for the radiologist. *Radiology*. 2020;295(1):16-17.
19. Qanadli SD, El Hajjam M, Vieillard-Baron A, et al. New CT index to quantify arterial obstruction in pulmonary embolism: comparison with angiographic index and echocardiography. *Am J Roentgenol*. 2001;176(6):1415-1420.
20. Podgorsak EB. Radiation oncology physics. *Vienna*. 2005: 123-271.
21. Bernheim A, Mei X, Huang M, et al. Chest CT findings in coronavirus disease-19 (COVID-19): relationship to duration of infection. *Radiology*. 2020;295(3):200463.
22. Caruso D, Zerunian M, Polici M, et al. Chest CT features of COVID-19 in Rome, Italy. *Radiology*. 2020;296(2):E79-E85.
23. Hani C, Trieu NH, Saab I, et al. COVID-19 pneumonia: a review of typical CT findings and differential diagnosis. *Diagn Interv Imag*. 2020;101(5):263-268. doi:10.1016/j.diii. 2020.03.014
24. Huda W. *Review of Radiologic Physics*. 4th ed. Wolters Kluwer Health; 2016:169.
25. Trott KR, Zschaecck S, Beck M. Radiation therapy for COVID-19 pneumopathy. *Radiother Oncol*. 2020;147:210-211.
26. Kirsch DG, Diehn M, Cucinoata FA, Weichselbaum R. Lack of supporting data make the risks of a clinical trial of radiation therapy as a treatment for COVID-19 pneumonia unacceptable. *Radiother Oncol*. 2020;147:217-220.
27. Lazzari G, Silvano G. RILI model and the Covid-19 pneumonia: the radiation oncologist point of view. *Radiother Oncol*. 2020; 147:222-223. doi:10.1016/j.radonc.2020.04.027